

University of Dayton

eCommons

Graduate Theses and Dissertations

Theses and Dissertations

2006

Electrocatalytic reduction of molecular oxygen at a graphite electrode coated with a cobalt (II) platinum (II) bimetallic porphyrin

Kalyan Ram Gadamsetti

University of Dayton

Follow this and additional works at: https://ecommons.udayton.edu/graduate_theses

Recommended Citation

Gadamsetti, Kalyan Ram, "Electrocatalytic reduction of molecular oxygen at a graphite electrode coated with a cobalt (II) platinum (II) bimetallic porphyrin" (2006). *Graduate Theses and Dissertations*. 2798.
https://ecommons.udayton.edu/graduate_theses/2798

This Thesis is brought to you for free and open access by the Theses and Dissertations at eCommons. It has been accepted for inclusion in Graduate Theses and Dissertations by an authorized administrator of eCommons. For more information, please contact mschlangen1@udayton.edu, ecommons@udayton.edu.

ELECTROCATALYTIC REDUCTION OF MOLECULAR OXYGEN AT A
GRAPHITE ELECTRODE COATED WITH A COBALT(II) /
PLATINUM(II) BIMETALLIC PORPHYRIN.

Thesis

Submitted to

The College of Arts and Sciences of the

UNIVERSITY OF DAYTON

In Partial Fulfillment of the Requirements for

The Degree

Master of Science in Chemistry

by

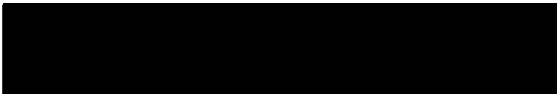
Kalyan Ram Gadamsetti

UNIVERSITY OF DAYTON

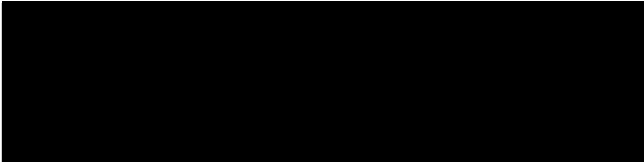
Dayton, Ohio

December, 2006


APPROVED BY:



Shawn M. Swavey, Ph.D., Assistant Professor,
Committee Chair



David W. Johnson, Ph.D., Associate Professor,
Committee Chair



Gary W. Morrow, Ph.D., Professor, Committee
Chair

ABSTRACT

ELECTROCATALYTIC REDUCTION OF MOLECULAR OXYGEN AT A GRAPHITE ELECTRODE COATED WITH A COBALT(II) / PLATINUM (II) BIMETALLIC PORPHYRIN.

Gadamsetti Kalyan Ram

University of Dayton

Advisor: Dr. S. M. Swavey

The porphyrin 5-(4-pyridyl)-10, 15, 20-(tris-3-methoxy-4-hydroxyphenyl)porphyrin (1) was synthesized by refluxing a solution of 3-methoxy-4-hydroxybenzaldehyde, 4-pyridinecarboxaldehyde and freshly distilled pyrrole in propionic acid. Column chromatography is used to separate porphyrin (1) from a mixture of 6 porphyrins. When the porphyrin is reacted with *cis*-Pt(DMSO)₂Cl₂ in dichloromethane at ambient temperature the platinum complex coordinates to the peripheral pyridyl group of the porphyrin. Cobalt inserts into *cis*-Pt(DMSO)-[5-(4-pyridyl)-10,15,20-(3-methoxy-4-hydroxyphenyl)porphyrin]Cl₂ when the Pt(II)-porphyrin complex is reacted with the cobalt(II) acetate and refluxed under nitrogen. Electropolymerization of Pt(II) and bimetallic Co(II)/Pt(II) porphyrins onto edge plane pyrolytic graphite (EPG) electrodes creates an electroactive surface capable of catalyzing the reduction of O₂ in acidic

solutions. When adsorbed onto EPG electrodes and anodically cycled in acidic solution the porphyrin complexes undergo an electrochemical-chemical-electrochemical (ECE) reaction. The newly formed electroactive surface is dependent on the proton concentration of the solution. Roughened EPG electrodes coated with the Co(II)/Pt(II) bimetallic porphyrin show a catalytic shift of 500 mV for the reduction of O_2 when compared to the reduction of O_2 at a bare EPG electrode. An additional catalytic shift of ca. 80 mV is observed for O_2 reduction at an EPG electrode coated with the Co(II)/Pt(II) porphyrin which has been oxidized in 1.0 M $HClO_4$. In addition to the added electrocatalysis a significant percentage of O_2 reduced at the oxidized Co(II)/Pt(II) EPG electrode is converted to H_2O as determined by rotating disk electrode measurements.

ACKNOWLEDGEMENTS

First and foremost, I would like to thank sincerely my research advisor, Dr. Shawn M. Swavey for his continuous support through out my masters program. He showed me different ways to approach a research problem and the need to be persistent to accomplish any goal. He has provided me with the freedom to learn on my own and I was always comfortable expressing my ideas to him. I would like to thank him for his patience and understanding which helped me in good preparation of my thesis. I would like to thank my parents for providing me an opportunity to study abroad. I would also like to thank the University of Dayton, Department of Chemistry for providing me excellent opportunity to start my career in the field of research and development. Finally and equally important, I would like to thank all faculty and staff for their support and help during these years.

TABLE OF CONTENTS

ABSTRACT.....	iii
ACKNOWLEDGEMENT.....	v
LIST OF ILLUSTRATIONS.....	viii
LIST OF TABLES.....	x
LIST OF SYMBOL/ABBREVIATIONS.....	xi

CHAPTER

I. INTRODUCTION.....	1
II. MATERIALS AND METHODS.....	9
Materials.....	9
Solution electrochemistry.....	10
Electronic Spectroscopy.....	10
Proton Spectroscopy	10
Preparations.....	10
Electrode preparation and adsorption of compound.....	13
III. RESULTS AND DISCUSSION.....	15
Synthesis of compounds and characterization.....	15
Electronic absorption spectroscopy.....	17
Solution Electrochemistry.....	19

	Electrode adsorption studies.....	21
	Electrocatalytic reduction of oxygen.....	25
IV.	CONCLUSIONS.....	31
V.	FUTURE DIRECTIONS.....	32
VI.	REFERENCES.....	33

LIST OF ILLUSTRATIONS

1. Schematic representation of a DMFC.....	2
2. Example of the simplest metalloporphyrin.....	4
3. Collmans dicobalt face to face Bis (porphyrin).....	5
4. Ansons Tetra-ruthenated cobalt(II) tetra-pyridylporphyrin.....	5
5. Nickel(II) tetrakis(3-methoxy-4-hydroxyphenyl)porphyrin, Ni(II)TMHPP.....	7
6. Structure of porphyrins and metalloporphyrins in this study.....	8
7. Synthesis of 5-(4-pyridyl)-10, 15, 20-(3-methoxy-4-hydroxyphenyl)porphyrin.....	15
8. Six porphyrins resulted by the reaction of two aldehydes and pyrrole.....	15
9. Electronic absorption spectra of the complexes in this study.....	18
10. Solution cyclic voltammogram of Complex 1.....	19
11. Solution cyclic voltammogram of Complex 2.....	20
12. Solution cyclic voltammogram of Complex 3.....	21
13. Cyclic voltammogram of complex 1 adsorbed onto an EPG electrode in 1.0M HClO ₄ solution vs. SCE.....	22
14. Cyclic voltammogram of complex 2 adsorbed onto an EPG electrode in 1.0M HClO ₄ solution vs. SCE.....	22
15. Cyclic voltammogram of complex 3 adsorbed onto an EPG electrode in 1.0M HClO ₄ solution vs. SCE.....	23

16. Electrochemical-Chemical-Electrochemical (ECE) reaction observed during anodic cycling in 1.0 M HClO ₄ coated with complex 1, 2 or 3.....	24
17. Cyclic voltammograms of complex 1 adsorbed onto a glassy carbon electrode after anodic cycling in 1.0 M HClO ₄ vs. SCE.....	25
18. O ₂ reduction at an EPG electrode coated with complex 3 prior to oxidation of the surface adsorbed complex and after anodic conditioning.....	26
19. Current-potential curves for the reduction of O ₂ at a rotating disk electrode coated with complex 3 prior to oxidation.....	27
20. Levich plot and Koutecky-Levich plots for current-potential curves of complex 3 prior to oxidation.....	27
21. Current-potential curves for the reduction of O ₂ at a rotating disk electrode coated with complex 3 after oxidation.....	29
22. Levich plot and Koutecky-Levich plots for current-potential curves of complex 3 after oxidation.....	29
23. Proposed structure of porphyrin for further study.....	32

LIST OF TABLES

1. Electronic absorption spectroscopy results for complexes in this study.....	18
--	----

LIST OF ABBREVIATIONS

PEM.....	Polymer Electrolyte Membrane.
PAFC.....	Phosphoric Acid Fuel Cell.
DMFC.....	Direct Methanol Fuel Cell.
AFC	Alkaline Fuel Cell.
MCFC.....	Molten Carbonate Fuel Cell.
SOFC	Solid Oxide Fuel Cell.
CO.....	Carbon monoxide.
NHE.....	Normal hydrogen electrode.
Ni(II)TMHPP.....	Nickel(II) tetrakis(3-methoxy-4-hydroxyphenyl)porphyrin.
EPG.....	Edge plane pyrolytic graphite pyrolytic graphite electrodes.
TBAP.....	Tetrabutyl ammonium hexafluorophosphate.
DMF.....	N, N' - dimethylformamide.
NMR.....	Nuclear magnetic resonance.
CDCl ₃	Deuterated chloroform.
SCE.....	Saturated calomel electrode.

CHAPTER 1

INTRODUCTION

Fuel cells are electrochemical devices that convert chemical energy into electrical energy.

A typical fuel cell consists of an electrolyte medium sandwiched between two electrodes (anode and cathode). The gaseous fuel is supplied continuously to the anode and an oxidant (usually air) is supplied continuously to the cathode and the electrochemical reactions take place at both electrodes to produce an electric current.¹

Fuel cells have high efficiency and cause low pollution to the environment. Fuel cells are often classified according to the kind of electrolyte they employ.² There are several types of fuel cells currently under development, each with its own advantages, limitations, and potential applications. Some of the types include Polymer Electrolyte Membrane (PEM), Phosphoric Acid Fuel Cell (PAFC), Direct Methanol Fuel Cells (DMFC), Alkaline Fuel Cells (AFC's), Molten Carbonate Fuel Cells (MCFC's), Solid Oxide Fuel Cells (SOFC's), Regenerative (Reversible) Fuel Cells.

DMFC is regarded as one of the most promising energy technologies in the 21st century. It is relatively new compared to that of fuel cells powered by pure hydrogen. The direct oxidation of methanol is a simplified way to convert the chemical energy of the methanol oxidation reaction to electricity. It is advantageous, only if the reaction leads to the formation of carbon dioxide and water at low anode potentials. Platinum is the

electrocatalyst used in DMFC but it is subjected to poisoning by CO; hence one of the challenges in developing DMFC is to find an inexpensive replacement for platinum to be able to oxidize methanol without poisoning its surface at such low potentials.³

In a DMFC, methanol is oxidized at the anode producing protons, carbon dioxide and electrons. The protons then diffuse across the electrolyte membrane to the cathode and the electrons are transported via an external circuit from anode to cathode providing power to external devices. When the electrons reach the cathode, they recombine with the protons that have passed across the membrane and reduce the oxygen to form water. The overall cell reaction thus corresponds to the combustion of methanol to produce carbon dioxide and water. An example of Direct Methanol Fuel Cell (DMFC) and the half-cell reactions are illustrated in Figure 1.

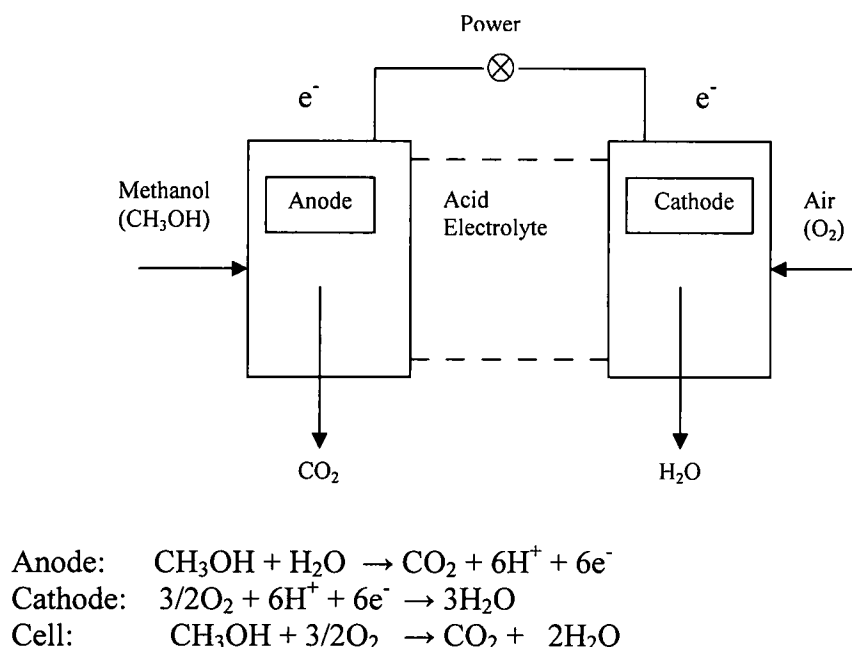
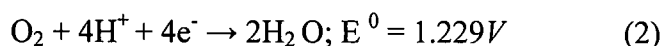
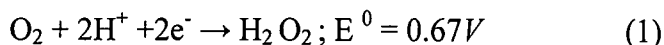


Figure 1. A simple schematic representation of a DMFC working in an acidic medium including the half reactions and cell reaction.³

The reduction of oxygen proceeds by a two-electron pathway to produce hydrogen peroxide or a direct four-electron pathway to give water in acidic solutions.⁴ In the two-electron pathway, oxygen is reduced to hydrogen peroxide by two electrons (1) The four-electron pathway is the reduction of oxygen to water directly without the production of peroxides (2).



The highest efficiency fuel cells seek to catalyze the direct reduction of dioxygen to water by four electrons at or near the thermodynamic potential of +1.23 V vs NHE at pH 0.⁵ This avoids the intermediate production of hydrogen peroxide which is a strong oxidant and is environmentally undesirable.⁶

Macrocyclic transition metal complexes have been extensively studied as dioxygen reduction catalysts⁷⁻⁸ but most of these are known to reduce dioxygen by only two electrons to form hydrogen peroxide and function only at rather low potentials.⁹ Studies involving the electrocatalytic reduction of oxygen by various synthetic metalloporphyrins have received a great deal of interest due to the possible use of these catalysts as electrode materials in energy conversion technologies, such as metal-air batteries and fuel cells.^{10,11}

A metalloporphyrin, Figure 2 is a compound, formed by the insertion of metal into the porphyrin center. A porphyrin is a heterocyclic macrocycle made from four pyrrole subunits linked on opposite sides through four methine bridges.

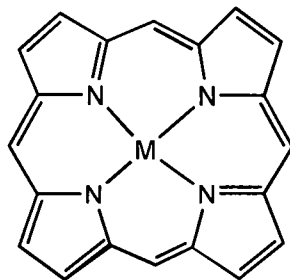


Figure 2. Example of the simplest metalloporphyrin 5,10,15,20-tetramethyleneporphyrin (where M = metals such as Co, Ni, Mn etc.) .

Among the various metalloporphyrins, cobalt porphyrins have been well studied and are well-known to exhibit electrocatalytic activity toward the reduction of O_2 ^{6, 12} although H_2O_2 instead of H_2O is the usual product. This is due to the release of H_2O_2 from the coordination sphere of the cobalt center immediately after its formation before it can be further reduced to water.¹³ Dimeric and monomeric iridium porphyrins have also been found to catalyze four electron reduction of oxygen at high potentials.^{6, 14}

Cofacial dicobalt porphyrins can catalyze the four electron reduction of dioxygen to water through direct interaction of both metal centers with the two oxygen atoms of O_2 .¹⁵⁻¹⁶ In a series of experiments, Collman and coworkers¹⁵ have studied the synthesis and characterization of the cofacial dicobalt porphyrin, Figure 3 and adsorbed it onto edge-plane graphite electrodes. This cofacial metalloporphyrin when tested for catalytic activity towards the electroreduction of dioxygen in aqueous acidic solution reduced O_2 directly to H_2O at relatively positive potentials.¹⁵

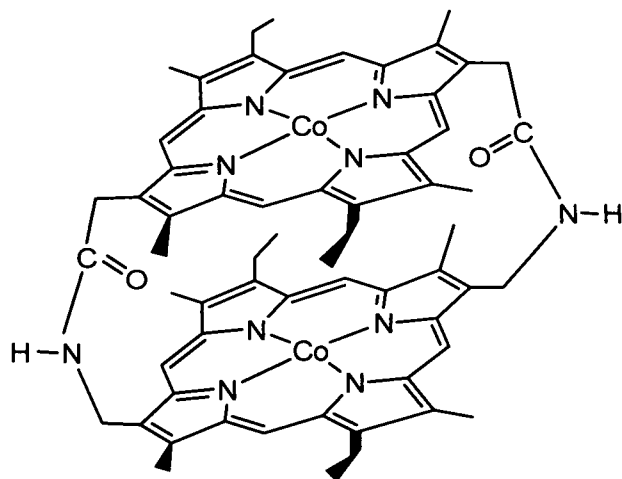


Figure 3. Collmans dicobalt face to face Bis (porphyrin).

In a series of studies Anson and coworkers have shown that the four-electron reduction of O_2 could be achieved by the coordination of three or four $Ru(II)(NH_3)_5$ groups to the ligand sites of (5,10,15,20 tetrakis(4-pyridyl)porphyrinato)cobalt(II) adsorbed onto pyrolytic graphite electrodes, Figure 4.¹⁷

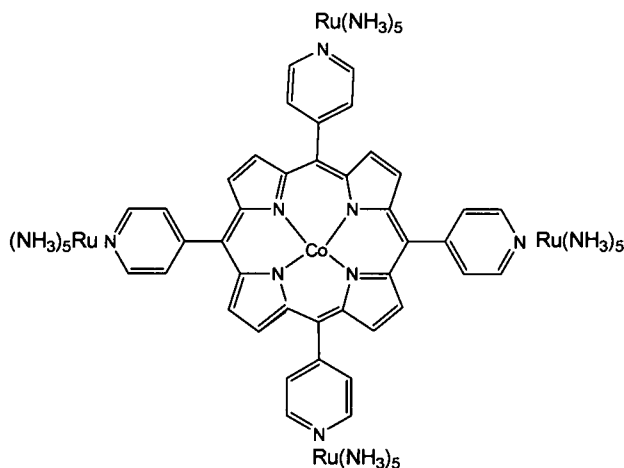


Figure 4. Ansons Tetra-ruthenated cobalt(II) tetra-pyridylporphyrin.¹⁷

It was initially thought intramolecular electron transfer from $Ru(II)$ to the $Co(II)$ center caused the four electron reduction of O_2 to water but later it was revealed that π back-bonding from the coordinated $Ru(II)(NH_3)_5$ groups through the pendant ligands into the

cobalt porphyrin ring was the primary factor responsible for the enhanced catalytic activity.^{18,19} Electrodes coated with monomeric multimetallic porphyrins of this type were found to be unstable in acidic solutions.¹⁷ Stability of many electrocatalysts have been improved by modification of the electrode surface.^{20,26,28}

Metalloporphyrins can be attached to solid electrode surfaces through various techniques. The most widely used techniques include adsorption, chemical reactions with previously functionalized electrodes, chemical reactions with a functionalized polymer, incorporation of the catalyst within the polymer film and electrochemical polymerization.²⁰ Metalloporphyrins when electropolymerised onto glassy carbon electrodes exhibit excellent stability and potential electrocatalytic ability. Iron, nickel and cobalt porphyrin based polymer films, when electropolymerized showed excellent electrocatalytic activities.²¹ Electrodes with modified films have shown diverse applications in the fields of electrocatalysis,²² electroanalysis,²³ biosensors,²⁴ and photodynamic therapy.²⁵ Electropolymerization can be achieved by cyclic voltammetry²⁶ or by galvanostatic methods and potentiostatic methods.²⁷ Chen Shen-Ming and Chen Ying-Lu²⁶ were able to electropolymerize manganese tetra(o-aminophenyl) porphyrin (MnTAPP) and produce stable and electrochemically active films on glassy carbon electrodes. In a different study, Cheng Shu-Hua and Yeh Chen-Yu²⁸ have synthesized two different types of porphyrin monomers (manganese-tetra(4-vinylphenyl)-porphyrin and manganese-tetra(4-stilbenyl)porphyrin) and electropolymerized the monomers onto glassy carbon electrodes. When cyclic voltammetry was carried out on these metallated porphyrins, there was an increase in amplitude of the peaks, which indicated the formation of a polymer film via electropolymerization.²⁶

Malinski and coworkers²⁰ have reported the synthesis, catalytic properties and oxidative electropolymerization of tetrakis(3-methoxy-4-hydroxyphenyl)porphyrin with Ni(II) as a central metal, (NiTMHPP, Figure 5).

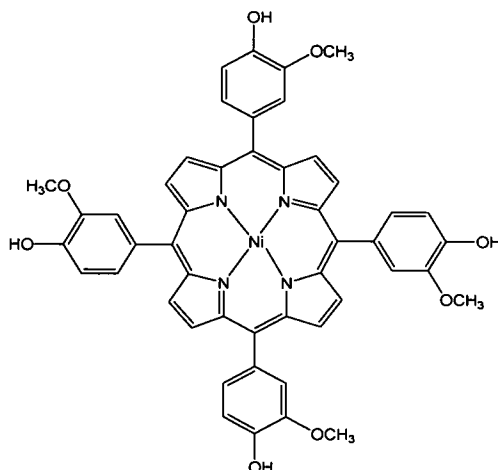


Figure 5. Nickel(II) tetrakis(3-methoxy-4-hydroxyphenyl)porphyrin, Ni(II)TMHPP.

In this study, they have observed the growth pattern for Ni(II)TMHPP in continuous scan cyclic voltammetry which indicated the formation of a conductive film on the surface of the glassy carbon electrode. The original oxidation peaks were noticed only during the first anodic scan. These peaks gradually decreased after the second and following scans and a redox couple appeared and increased after each scan. This multiple scan voltammogram indicated the formation of stable films on glassy carbon electrodes. Polymeric NiTMHPP electrodes when transferred to aqueous 0.1M NaOH showed only one reversible couple. Malinski and coworkers concluded that the current and reversibility of the redox couple strongly depend on the pH and composition of the supporting electrolyte.

Further evidence for the polymerization process was shown by observing the shift in the Soret band of the polymeric porphyrin film compared to the monomer during the

electrochemical oxidation of NiTMHPP in aqueous 0.1M NaOH on indium oxide coated transparent electrodes using thin layer absorption spectroscopy. According to Malinski and coworkers, continued growth of the film was apparently due to electrochemical oxidation of molecules in the subsequent layer, by oxidative cycling of surface molecules followed by further reaction with initial parent molecule from the solution resulting in further polymerization. The electrodes of poly-NiTMHPP have been used as electrocatalysts for the oxidation of methanol, water and hydrazine.²⁰

The present thesis describes the synthesis and solution characterization of 5-(4-pyridyl)-10,15,20-(3-methoxy-4-hydroxyphenyl)porphyrin (**1**), *cis*-Pt(DMSO)-[5-(4-pyridyl)-10,15,20-(3-methoxy-4-hydroxyphenyl)porphyrin]Cl₂ (**2**) and *cis*-Pt(DMSO)-[5-(4-pyridyl)-10,15,20-(3-methoxy-4-hydroxyphenyl)porphyrinatocobalt(II)]Cl₂ (**3**), Figure 6 by UV-Vis spectroscopy, cyclic voltammetry and ¹H NMR spectroscopy. When these porphyrins (Figure 6) were adsorbed onto pyrolytic graphite (EPG) electrodes and studied by

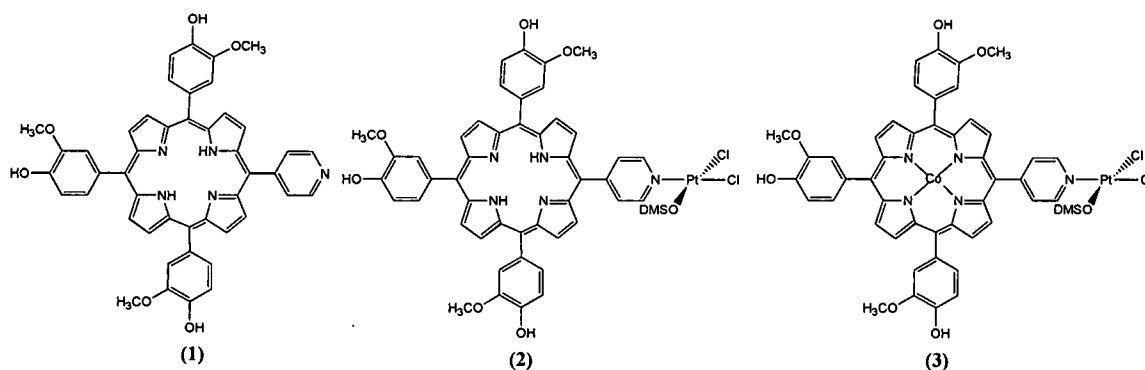


Figure 6. Structure of porphyrins and metalloporphyrins in this study.

voltammetry in acidic solutions, a redox active polymer was formed. Enhanced electrocatalytic reduction of oxygen was observed at electrodes modified with complex (**3**).

CHAPTER 2

EXPERIMENTAL SECTION

Materials

All reagents were analytical grade unless stated otherwise. 3-methoxy-4-hydroxybenzaldehyde, 4-pyridinecarboxaldehyde, propionic acid, methanol, N, N'-dimethylformamide (DMF), tetrabutyl ammonium hexafluorophosphate, TBAP, used as supporting electrolyte for electrochemistry, and N, N' dimethyl formamide (extra dry <50 ppm H₂O) (for electrochemistry) were used from Acros Organics. Methylene chloride, perchloric acid, cobalt (II) acetate and (60-200 mesh) silica gel were used from Fisher Scientific. Materials used to prepare buffer solutions were sodium phosphate monobasic, (NaH₂PO₄), sodium phosphate dibasic, (Na₂HPO₄), phosphoric acid, (H₃PO₄), acetic acid, (CH₃COOH) and sodium acetate, (CH₃COONa) obtained from Acros Organics. All the reagents were used without further purification. *cis*-dichlorobis(dimethylsulfoxide)platinum(II) (*cis*-Pt(DMSO)₂Cl₂)²⁹ was prepared according to literature procedure. Pyrrole (Aldrich) was vacuum distilled prior to use. The buffer solutions and their pH values, measured to ± 0.01 at 25 °C using a Denver Instrument Ultrabasic pH meter calibrated with standard pH 4.00 and 10.00 buffer solutions (Fisher), were as follows: 0.2 M NaH₂PO₄, 0.05 M H₃PO₄ (2.61); 0.24 M CH₃COOH, 0.05 M CH₃COONa (3.73); 0.2 M CH₃COONa, 0.05 M CH₃COOH (4.97);

0.2 M NaH_2PO_4 , 0.05 M Na_2HPO_4 (6.19). Elemental analyses were performed by Atlantic Microlab, Norcross, GA.

Solution Electrochemistry

Solution cyclic voltammograms were recorded using a one-compartment, three electrode cell, (model 630A Electrochemical analyzer from CH-Instruments) equipped with a platinum wire auxiliary electrode. The working electrode was a 2.0 mm diameter glassy carbon electrode from CH-Instruments. The working electrode was polished first using 0.30 μ followed by 0.05 μ alumina polish (CH-Instruments) and then sonicated for 5 sec and tapped dry with a kimwipe prior to use. Potentials were referenced to a saturated calomel electrode (SCE). The supporting electrolyte was 0.1 M TBAP and the measurements were made in extra dry DMF.

Electronic Spectroscopy

UV-Vis spectra were recorded at room temperature using a Shimadzu 1501 photodiode array spectrophotometer with 2 nm resolution. Samples were run in UV-grade CH_2Cl_2 in 1 cm quartz cuvettes.

Proton NMR Spectroscopy

^1H NMR spectra were recorded on a Bruker 300 MHz spectrophotometer using deuterated chloroform (CDCl_3) as the solvent and tetramethylsilane (TMS) as the internal standard.

Preparations

Synthesis of 5-(4-pyridyl)-10, 15, 20-(3-methoxy-4-hydroxyphenyl)porphyrin

7.5 g (0.049 moles) of 3-methoxy-4-hydroxybenzaldehyde and 1.6 mL (0.015 moles) of 4-pyridinecarboxaldehyde were combined in 100 mL of propionic acid and heated at

reflux for 5 min. 4.4 mL (0.066 moles) of freshly distilled pyrrole and 25 mL of propionic acid were added to this solution and refluxed for 1 hr. The reaction mixture was cooled to room temperature and added to a solution containing 200 mL of 50:50 methanol: ammonium hydroxide solution which was prepared and cooled in an ice bath. The slurry was placed in a refrigerator for one day to allow precipitation. When the precipitate was formed, the slurry was filtered and washed 3 times with 100 mL portions of methanol. Soxhlet extraction was carried out with approximately 250 mL of methanol for 24 hrs. Then the purple powder in the thimble was extracted using 200 mL of ethyl acetate by soxhlet extraction for 24 hrs. The filtrate was collected and the solvent was partially removed under reduced pressure until nearly 70-80 mL of solution was present. It was then gravity filtered. The resulting solution was chromatographed on silica gel using wet column chromatography with pure ethyl acetate as the eluent. The second red band off the column was collected and the solvent was removed under reduced pressure. The product yield was 75 mg.

The methanol extract was allowed to dry and was dissolved in 50 mL of pure ethyl acetate. The resulting solution was chromatographed on silica gel using wet column chromatography with pure ethyl acetate as the eluent and the second red band was collected and the solvent was removed under reduced pressure. The product yield was 55 mg. The total yield of the product was 130 mg. (0.17 mmol, 1.15% yield).

UV-Vis (CH_2Cl_2) λ_{max} (nm) [$\epsilon \times 10^{-4}$ ($\text{M}^{-1}\text{cm}^{-1}$)]: 425 [16.56], 519 [1.13], 557 [0.78], 594 [0.46], 651 [0.43]. ^1H NMR (300 MHz, CDCl_3 , TMS): δ 9.03 (2H, d, 2,6-pyridyl), 8.95 (6H, m, pyrrole β), 8.79 (2H, d, pyrrole β), 8.18 (2H, d, 3,5-pyridyl), 7.79 (6H, m, 2{3-methoxy-4-hydroxyphenyl}) and 6{3-methoxy-4-hydroxyphenyl}), 4.01 (9H, s, *m*-

methoxy), -2.79(2H, s, internal pyrrole). [C₄₆H₃₅N₅O₆·1.5H₂O] Anal. Calcd (%): C, 70.76; H, 4.91; N, 8.97. Found: C, 70.97; H, 5.06; N, 8.58.

Synthesis of *cis*-Pt(DMSO)-[5-(4-pyridyl)-10,15,20-(3-methoxy-4-hydroxyphenyl)porphyrin]Cl₂

To a solution containing 70 mg (0.093 mmol) of 5-(4-pyridyl)-10, 15, 20-(3-methoxy-4-hydroxyphenyl)porphyrin in 20 mL of dichloromethane was added 39 mg (0.093 mmol) of *cis*-dichlorobis(dimethylsulfoxide)platinum(II) and the solution was stirred at ambient temperature for 4 hrs. The resulting solution was chromatographed on silica gel using dry column chromatography with a 50:50 ethyl acetate/chloroform mixture as the eluent. The first red band off the column was collected and the solvent was removed under reduced pressure. The product yield was 65 mg. (0.056 mmol, 61% yield).

UV-Vis (CH₂Cl₂) λ_{max} (nm) [ε × 10⁻⁴ (M⁻¹cm⁻¹): 427 [21.2], 521 [1.50], 560 [1.12], 595 [0.56], 653 [0.60]. ¹H NMR (300 MHz, CDCl₃, TMS): δ 9.19 (2H, d, 2,6-pyridyl), 8.94 (4H, s, pyrrole β), 8.79 (2H, d, pyrrole β), 8.28 (2H, d, 3,5-pyridyl), 7.76 (6H, m, 3-methoxy-4-hydroxyphenyl), 4.01 (9H, s, p-methoxy), 3.62 (6H, s, DMSO), -2.79(2H, s, internal pyrrole). [C₄₈H₄₁N₅O₇SCl₂Pt·3H₂O] Anal. Calcd (%): C, 50.05; H, 4.11; N, 6.08. Found: C, 50.04; H, 3.85; N, 5.94.

Synthesis of *cis*-Pt(DMSO)-[5-(4-pyridyl)-10,15,20-(3-methoxy-4-hydroxyphenyl)porphyrinatocobalt(II)]Cl₂

To a solution of *cis*-Pt(DMSO)-[5-(4-pyridyl)-10,15,20-(3-methoxy-4-hydroxyphenyl)porphyrin]Cl₂ (70 mg, 0.0637 mmol) in chloroform (20 mL) was added a solution of cobalt acetate (32 mg, 0.128 mmol) in methanol (1 mL). After 30 min. of heating at reflux under nitrogen, the mixture was rotovapped, concentrated to about 1 mL

and diluted with 10 mL of water. It was filtered and washed with water to get the precipitate. The experimental yield is 35 mg. (0.03 mol, 47% yield).

UV-Vis (CH_2Cl_2) λ_{max} (nm) [$\epsilon \times 10^{-4}$ ($\text{M}^{-1}\text{cm}^{-1}$)]: 418 [23.2], 532 [1.44],
[$\text{C}_{48}\text{H}_{39}\text{N}_5\text{O}_7\text{SCl}_2\text{CoPt}\cdot 5\text{H}_2\text{O}$] Anal. Calcd (%): C, 46.31; H, 3.97; N, 5.63; S, 2.58.
Found: C, 46.00; H, 3.60; N, 5.73; S, 3.12.

Electrode preparation and adsorption of compound

Bipotentiostat model AFCBP1 and AFMSRX rotator from Pine Instrument Co. were used to record the cyclic voltammograms and to carry out the rotating disc experiments. The edge plane pyrolytic graphite electrode (EPG electrode, AFE3T 5.0 mm diameter, Pine Instrument Co.) was initially polished using alpha micropolish alumina 5.0 micron particle size and then with gamma micropolish II alumina of 0.05 micron particle size (Buehler Co.) on a Buehler polishing cloth with deionised water as lubricant. It was then rinsed with deionised water and then sonicated (Branson co. sonicator) in deionised water for 10 sec. After sonicating, the electrode surface was roughened using 600 grit sandpaper. It was rinsed using deionised water, tapped dry with a kimwipe. 5-15 μL aliquots of 1.0 mM acetone solutions of the porphyrins and metalloporphyrins were adsorbed onto the EPG electrode using 50 μL syringe (Hamilton Co.) and allowed for the solvent to evaporate at room temperature (20 $^{\circ}\text{C}$). The electrodes were finally rinsed with deionised water and tapped dry with a kimwipe. The cyclic voltammetric experiments were carried out in a 3-electrode system using an edge plane pyrolytic graphite electrode as the working electrode, platinum wire as the counter electrode and a saturated calomel electrode as the reference electrode. Electrochemical studies were performed in 1.0 M

perchloric acid solutions. Oxygen reduction studies were performed in a similar solution which was purged with air for approximately 15 min. prior to the experiment.

CHAPTER 3

RESULTS AND DISCUSSION

Synthesis of compounds and characterization

Two different aldehydes 3-methoxy-4-hydroxybenzaldehyde and 4-pyridinecarboxaldehyde were used along with pyrrole for the synthesis of porphyrin 1, Figure 7.

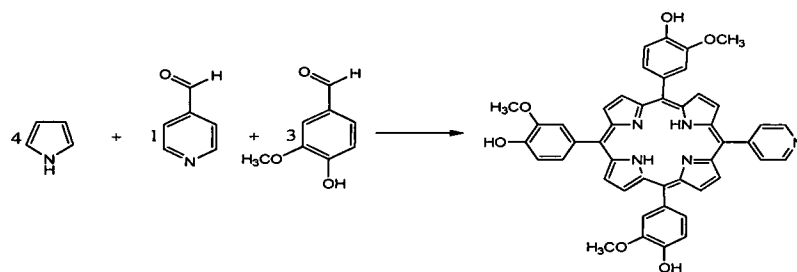


Figure 7. Synthesis of 5-(4-pyridyl)-10, 15, 20-(3-methoxy-4-hydroxyphenyl)porphyrin.

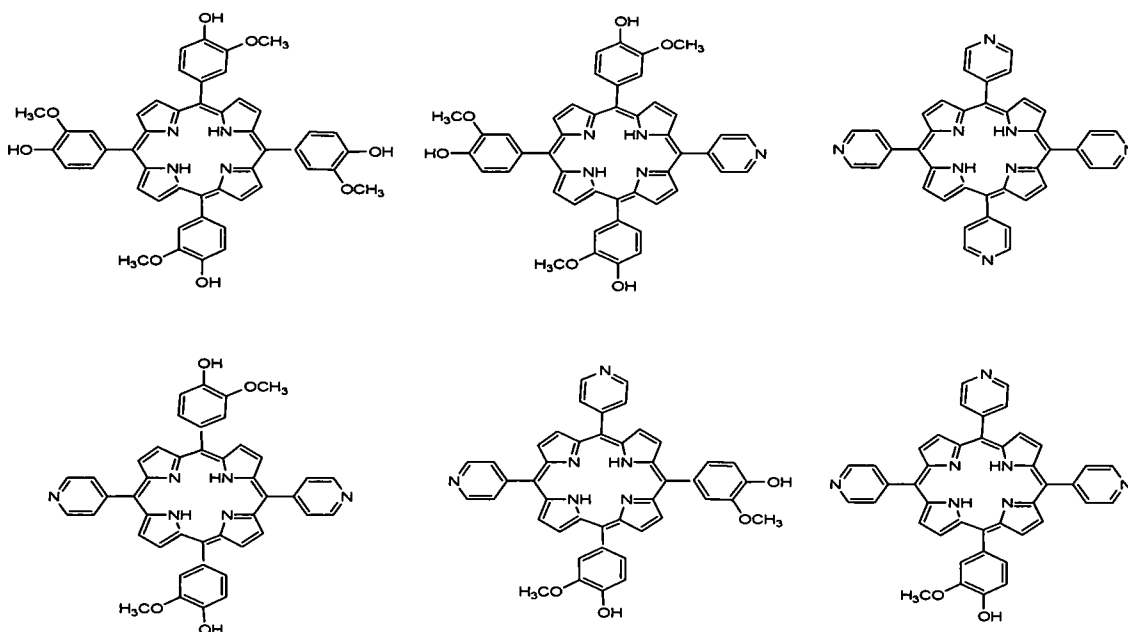


Figure 8. Six porphyrins resulted by the reaction of two aldehydes and pyrrole.

Synthesis of porphyrin **1** was complicated by formation of polymeric byproducts and a statistical distribution of other porphyrins, Figure 8. Two separate methods were carried out to purify compound **1**. In one method the methanol extract which was collected after soxhlet extraction was column chromatographed and the second band off the column was collected, the product yield was 0.3 %. In another method soxhlet extraction was carried out with ethylacetate and the resulting extract was column chromatographed collecting the second band, the product yield was 0.4 %. In both methods, streaking on the column prevented clean separation of the porphyrins. It was discovered that if the compound left in the thimble after methanol extraction was extracted with ethyl acetate and then chromatographed, clean separation of the desired porphyrin could be obtained.

Porphyrin **2** was synthesized by adding equal moles of porphyrin **1** and *cis*-Pt(DMSO)₂Cl₂ in dichloromethane.³⁰ The solution was stirred at ambient temperature for 4 hours and chromatographed. Coordination of the Pt(II) moiety was identified by ¹H NMR. Comparison of the methoxy protons associated with the porphyrin which occur as singlets at 4.01 ppm and the protons associated with the methyl groups of the dimethylsulfoxide (DMSO) ligand which occur as a singlet at 3.62 ppm indicated coordination of the Pt(II) moiety, with an integrated ratio of 3:2 respectively.

Insertion of Co(II) into the porphyrin-Pt(II) complex **2**³⁰ was achieved by adding a solution of porphyrin **2** dissolved in chloroform to a solution of cobalt(II) acetate dissolved in methanol and the reaction mixture was refluxed under nitrogen. It was then concentrated and extracted with water and dried. This lead to good yields of the bimetallic Co(II) / Pt(II) porphyrin. Repeated attempts to insert Co(II) into the porphyrin (**1**) resulted in an insoluble product.

Electronic absorption spectroscopy

In the UV-Vis absorption spectrum, the highly conjugated porphyrin macrocycle shows intense absorption in the form of characteristic Soret band at around 400 nm followed by weak absorptions at longer wavelengths (450 – 700 nm) in the form of several Q-bands. Insertion of a metal into the porphyrin centre or protonation of two of the inner nitrogen atoms also changes the visible absorption spectrum. Variations of the peripheral substituents on the porphyrin ring often cause minor changes to the intensity and wavelength of these absorptions. Comparison of electronic transitions associated with complexes **1-3** in CH₂Cl₂ is illustrated in Figure 9. A Soret band at 425 nm and four Q-bands at lower energy were observed for complex **1**, dotted line Figure 9. A slight shift in the Soret band from 425 to 427 nm is observed with increased intensity of the absorption band upon coordination of Pt(DMSO)Cl₂ to the pyridyl group, dashed line Figure 9. The Q-bands associated with complex **2** also experience a similar shift to lower energy by 2 to 3 nm. When Co(II) was inserted into the porphyrin center of complex **2**, due to increase of symmetry, the four Q-bands associated with the porphyrin **2** collapsed into a single band at 532 nm. In addition the Soret band shifted to 418 nm, solid line Figure 9. The assignments for these transitions are indicated in Table 1.

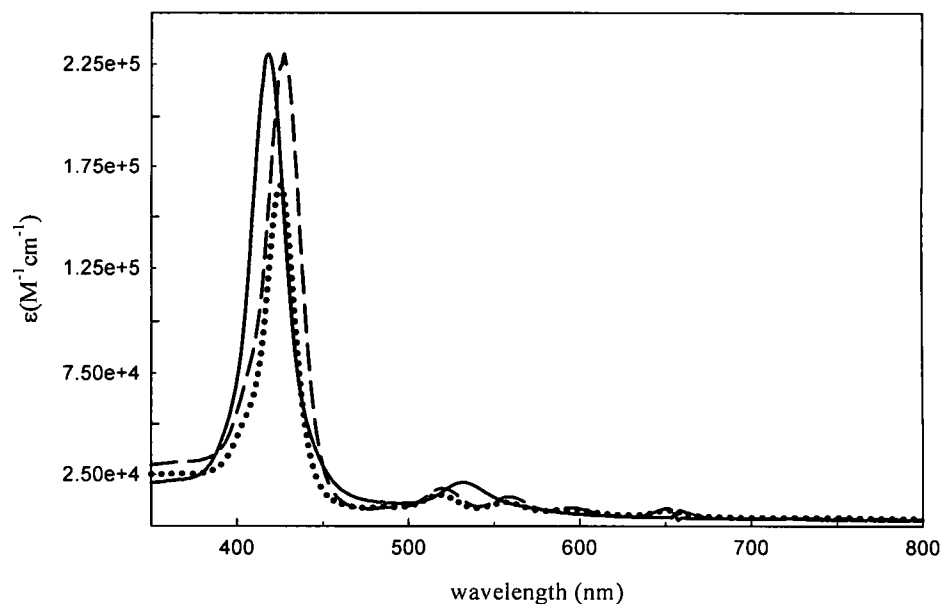


Figure 9. Electronic absorption spectra in dichloromethane at room temperature in 1 cm quartz cells for complex 1 (·····), complex 2 (-----) and complex 3 (———).

Complex	λ_{max} (nm)	$\epsilon \times 10^4$ ($\text{M}^{-1} \text{cm}^{-1}$)	Assignment
1	425	16.6	Soret ($\pi - \pi^*$)
	519	1.13	Q-band
	557	0.79	Q-band
	594	0.46	Q-band
	651	0.42	Q-band
2	427	21.2	Soret ($\pi - \pi^*$)
	521	1.5	Q-band
	560	1.12	Q-band
	595	0.56	Q-band
	653	0.59	Q-band
3	418	23.2	Soret ($\pi - \pi^*$)
	532	14.4	Q-band

Table 1. Electronic absorption spectroscopy results for complexes 1-3. Electronic spectra were taken in 1 cm quartz cells in dichloromethane.

Solution Electrochemistry

Solution cyclic voltammograms were recorded using a one-compartment, three electrode cell, equipped with a platinum wire auxiliary electrode. A glassy carbon electrode used as the working electrode was polished first using 0.30 μ followed by 0.05 μ alumina polish and then sonicated for 5 sec and tapped dry with a kimwipe prior to use. Potentials were referenced to a SCE electrode. The supporting electrolyte was 0.1 M TBAP and the measurements were made in extra dry DMF.

Figure 10 shows the cyclic voltammogram of complex **1**. In the anodic direction, there is an irreversible oxidation process at $E_{pa} = 0.93$ V versus SCE which is due to formation of a porphyrin radical cation, which undergoes a chemical reaction following its formation. The cathodic region of the voltammogram for **1** shows a quasireversible redox couple with $E_{1/2} = -1.06$ V vs SCE, which can be associated with reduction of the porphyrin ring to form the monoanion.³¹

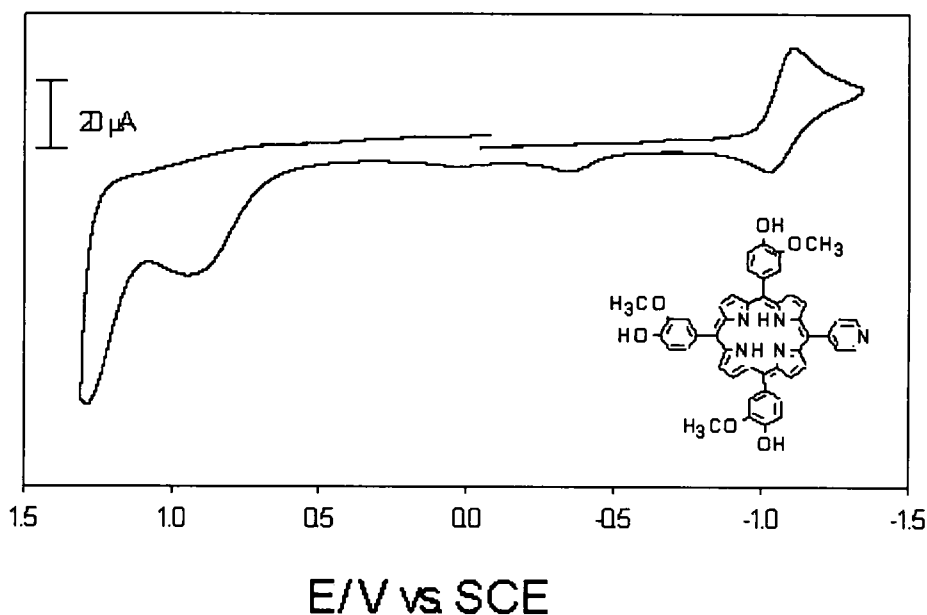


Figure 10. Solution cyclic voltammogram of Complex **1** vs. SCE. Working electrode is glassy carbon with a scan rate of 100 mv/ sec under a nitrogen atmosphere.

Figure 11 shows the cyclic voltammogram of complex **2**. In the anodic direction, the irreversible oxidation associated with porphyrin cation formation is shifted to more positive potentials ($E_{pa} = 1.02$ V) by the Pt(II) moiety. An irreversible reduction process at $E_{pc} = -1.03$ V vs. SCE, Figure 11 is associated with the Pt(II) metal center and is assigned to the reduction of Pt(II) to Pt(I) based on voltammetric studies of square planar Pt(II) complexes in aprotic media.³² In the cathodic direction, a quasireversible reduction of the porphyrin at $E_{1/2} = -1.06$ V vs. SCE, Figure 10 becomes irreversible and shifted to more negative potentials, $E_{pc} = -1.18$ V, upon coordination of Pt(DMSO)Cl₂, Figure 11.

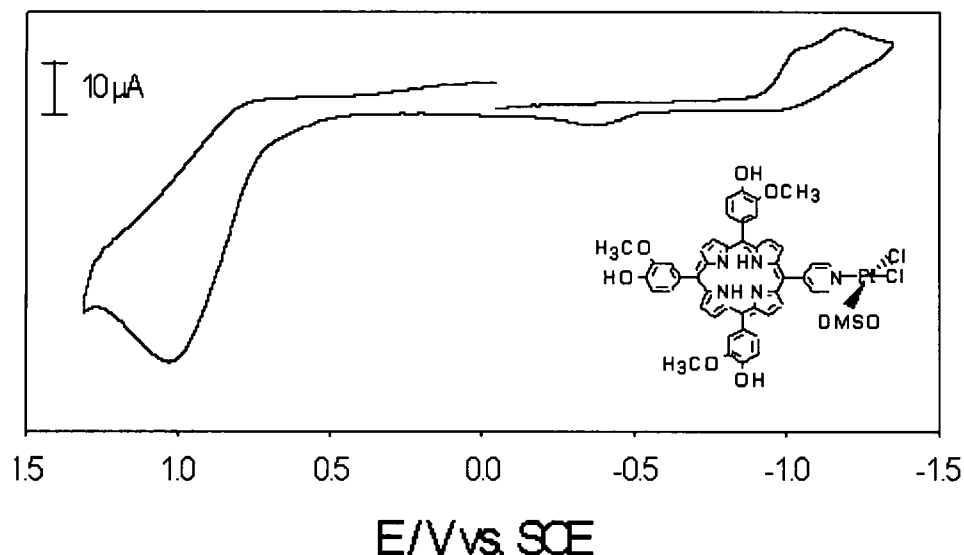


Figure 11. Solution cyclic voltammogram of Complex **2** vs. SCE. Working electrode is glassy carbon with a scan rate of 100 mv/ sec under a nitrogen atmosphere.

Formation of the porphyrin cation occurs at $E_{pa} = 1.02$ V for Complex **3**, Figure 12. Upon insertion of Co(II) into the porphyrin center of complex **2**, the reduction of Pt(II) and the porphyrin is shifted to more negative potentials. A reversible redox couple at $E_{1/2} = -0.76$ V is observed for the Co(II)-Pt(II) complex **3**, Figure 12. This can be attributed to the

Co^{II/I} redox couple.³³ The Co^{III/II} couple was not observed due to slow electron transfer kinetics in DMF.³³

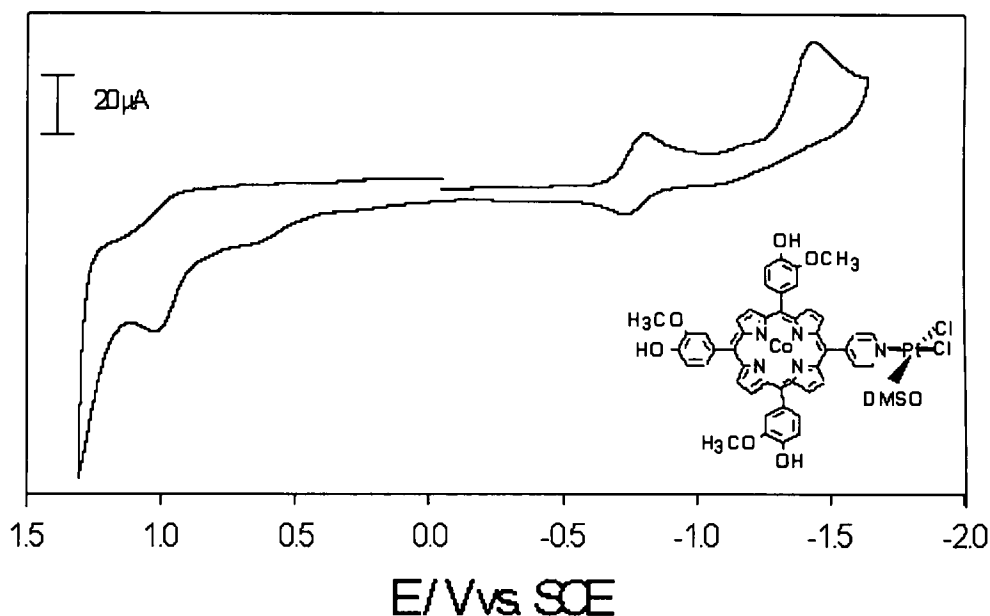


Figure 12. Solution cyclic voltammogram of Complex **3** vs. SCE. Working electrode is glassy carbon with a scan rate of 100 mV/sec under a nitrogen atmosphere.

Electrode adsorption studies

After scoring the surface of an EPG electrode, using 600 grit sandpaper, 5-15 μL aliquots of 1 mM acetone solutions of the porphyrin were adsorbed onto the electrode allowing the solvent to evaporate at room temperature. Electrochemical properties of the complexes adsorbed onto an EPG electrode were studied in 1.0 M HClO_4 .

When an EPG electrode coated with complex **1** is cycled in 1.0 M HClO_4 , an irreversible oxidation wave on the first anodic scan is observed with $E_{\text{pa}} = 0.77$ V vs. SCE, Figure 13. Upon reversing the scan direction, a reduction wave IIa coupled to an oxidation wave IIb is observed. The reduction and oxidation wave together form the

quasireversible redox couple, IIa/IIb, Figure 13, with an $E_{1/2} = 0.57$ V. This new redox couple is the result of an electrochemical-chemical-electrochemical (ECE) reaction.²⁰

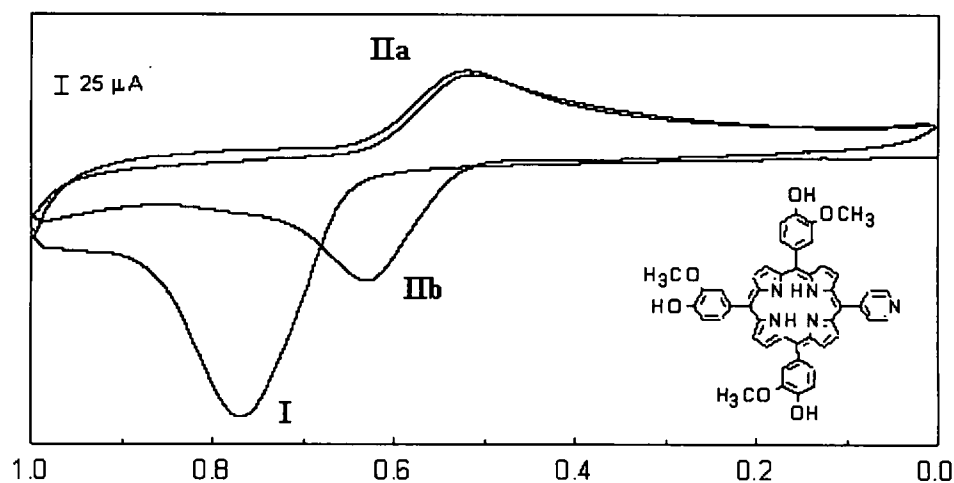


Figure 13. Cyclic voltammogram of complex 1 adsorbed onto an EPG electrode in 1.0 M HClO₄ solution vs. SCE. Scan rate = 100 mv / sec.

Figure 14 illustrates the cyclic voltammogram of complex 2 adsorbed onto an EPG electrode in 1.0 M HClO₄ solution. Oxidation of the adsorbed complex at $E_{pa} = 0.81$ V leads to the formation of a quasireversible redox couple, IIa/IIb, Figure 14, with an $E_{1/2} = 0.60$ V.

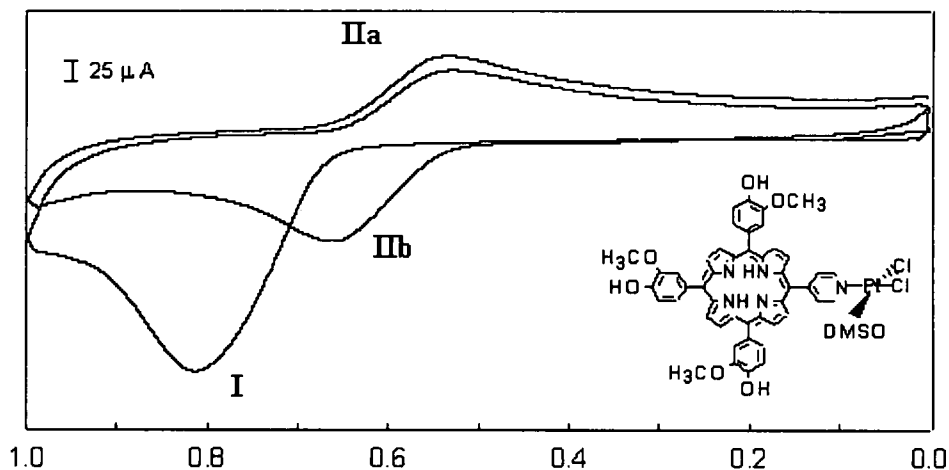


Figure 14. Cyclic voltammogram of complex 2 adsorbed onto an EPG electrode in 1.0 M HClO₄ solution vs. SCE. Scan rate = 100 mv / sec.

Anodic cycling in 1.0 M HClO₄ with an EPG electrode coated with the Co(II)-Pt(II) porphyrin, Complex **3** shows an irreversible oxidation wave with $E_{pa} = 0.76$ V vs. SCE, I, Figure 15. The new redox couple formed after oxidation, IIa / IIb, $E_{1/2} = 0.57$ V is similar to the redox process of complex **1** and **2**. This suggests two things, first the oxidation process and subsequent chemical reaction are associated with porphyrin most likely the 3-methoxy-4-hydroxy phenyl substituents, second the presence of Pt(II) and Co(II) have little or no effect on this mechanism.

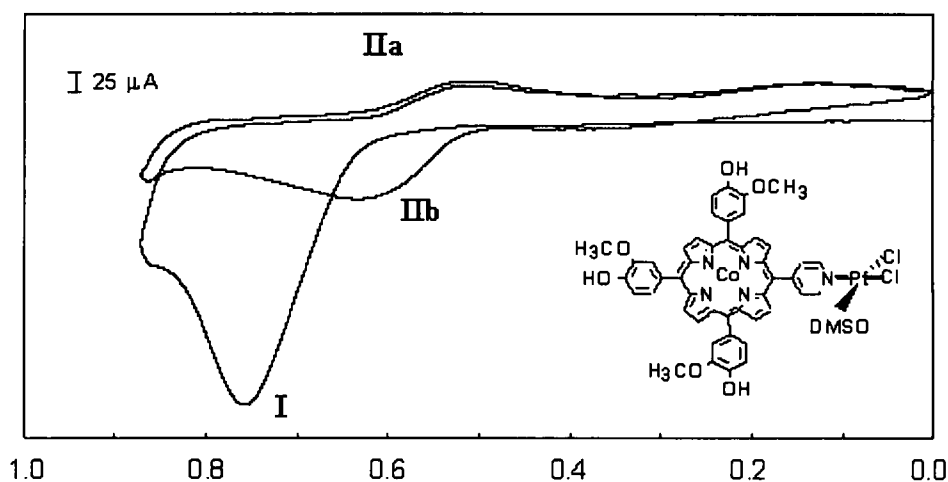


Figure 15. Cyclic voltammogram of complex **3** adsorbed onto an EPG electrode in 1.0 M HClO₄ solution vs. SCE. Scan rate = 100 mv / sec.

The ECE mechanism describes a process in which an electrochemical step is followed by a chemical step which is then followed by an electrochemical step. The ECE mechanism for the complexes **1**, **2** and **3** during anodic cycling in 1.0 M HClO₄ solution is illustrated in Figure 16. In the first step, the 3-methoxy-4-hydroxyphenyl peripheral groups undergo two electron oxidation. It is followed by a chemical reaction most likely the demethylation of the methoxy substituents leading to a highly reactive quinonoid

structure capable of reacting to form a redox active film on the electrode surface.²⁰ The next step is an electrochemical step where the quinone complex undergoes two electron two proton reduction to hydroquinone which is a reversible reaction.

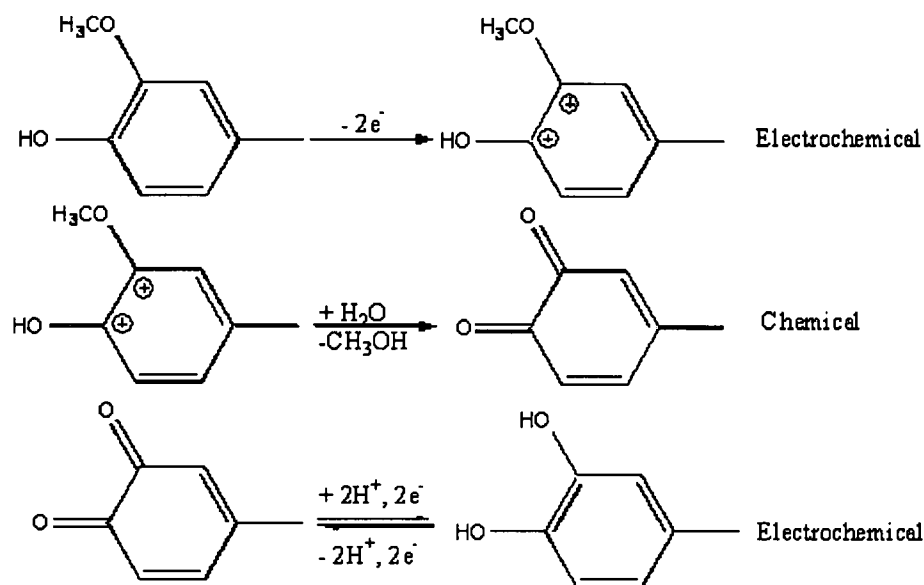


Figure 16. Electrochemical-Chemical-Electrochemical (ECE) reaction observed during anodic cycling in 1.0 M $HClO_4$ coated with complexes 1, 2 and 3.

The dependence of the newly formed redox couples on the pH of the electrolyte solution was studied by adsorbing the complexes onto glassy carbon electrodes and cycling anodically in 1.0 M $HClO_4$ solution. The electrode was removed and placed into a buffer solution of known pH and cycled through the potential region associated with the newly formed redox couple. Figure 17 illustrates the results of a pH study conducted on a glassy carbon electrode coated with complex 1 after it had been oxidized in 1.0 M $HClO_4$. As the $[H^+]$ decreases, the redox couple shifts to lower potentials. A plot of $E_{1/2}$ values vs. pH, inset Figure 17, is linear with a slope of -0.064 V/pH unit consistent with a $1e^-/1H^+$

process. Similar studies of complexes **2** and **3** give linear $E_{1/2}$ vs. pH relationships with slopes of -0.059 V and -0.054 V per pH unit respectively.³⁴

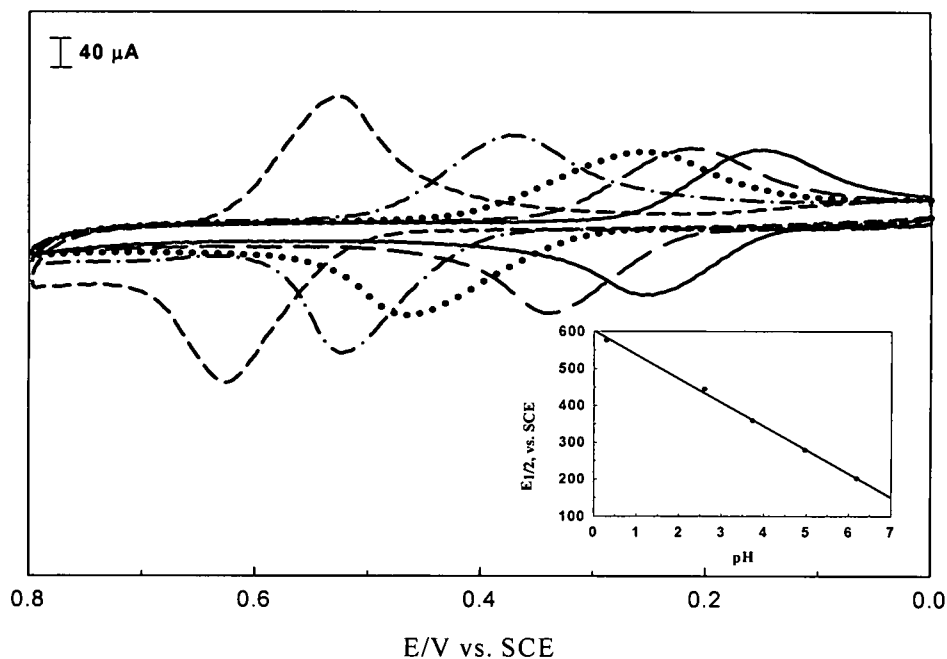


Figure 17. Cyclic voltammograms of complex **1** adsorbed onto a glassy carbon electrode after anodic cycling in 1.0 M HClO_4 vs. SCE.

Electrocatalytic reduction of Oxygen

The electrocatalytic reduction of O_2 in 1.0 M HClO_4 was studied at an EPG electrode coated with the Co(II)/Pt(II) porphyrin **3** using cyclic voltammetry and rotating disk electrode (RDE) voltammetry.

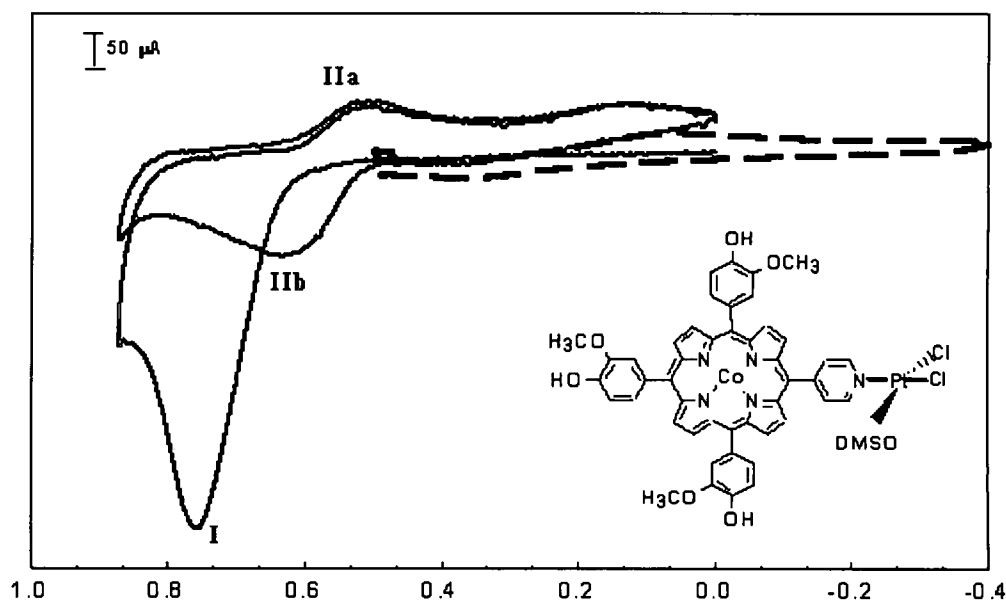


Figure 18. O_2 reduction at an EPG electrode coated with complex **3** in air saturated 1.0 M HClO_4 prior to oxidation of the surface adsorbed complex (-----) and after anodic conditioning (—), scan rate = 100 mV/s, referenced to the saturated calomel electrode (SCE).

Reduction of O_2 at a bare EPG electrode in air saturated 1.0 M HClO_4 occurs with an $E_{1/2} = -0.35$ V vs. SCE. An EPG electrode coated with the Co(II)/Pt(II) porphyrin **3** in air saturated 1.0 M HClO_4 reduces O_2 with an $E_{1/2} = 0.14$ V vs. SCE, dotted line Figure 18, a catalytic shift of 500 mV compared to the bare EPG electrode. A catalytic shift of nearly 600 mV when compared to the bare EPG electrode is observed for O_2 reduction at an EPG electrode coated with **3** after oxidation of the surface confined complex, solid line Figure 18.

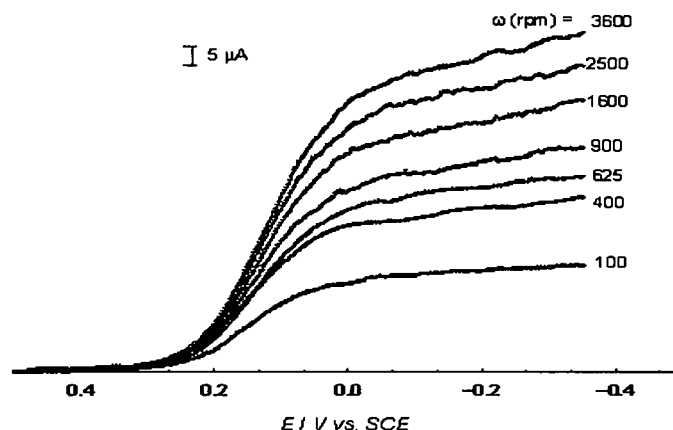


Figure 19. Current-potential curves in air saturated 1.0 M HClO_4 solution for the reduction of O_2 at a rotating disk electrode coated with complex **3** prior to oxidation at 1.0 V with a scan rate of 5 mV/sec .

Figure 19 illustrates the results of the RDE experiment performed on an EPG electrode coated with **3** in air saturated 1.0 M HClO_4 prior to oxidation of the adsorbed complex. A plot of the diffusion-limited current density versus the square root of the rotation rate, the Levich plot, indicates a deviation from linearity at higher rotation rates attributed to a potential independent rate limiting step,¹³ Figure 20a.

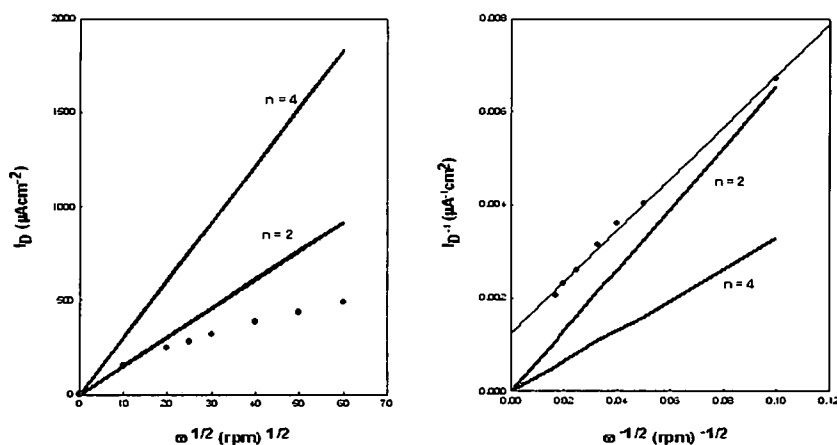


Figure 20. (a) Levich plot of plateau current vs. square root of the rotation rate for the current-potential curves of complex **3**., Figure 19. (b) Koutecky-Levich plot of the inverse of the plateau current vs. inverse of square root of the rotation rate for current-potential curves of complex **3**., Figure 19. The theoretical two electron and four electron lines are marked $n = 2$ and $n = 4$, respectively.

The Koutecky-Levich plot, Figure 20b, relates the plateau current density to the rotation rate using equation 1.³⁵

$$1/I_L = 1/I_k + 1/B\omega^{1/2} \quad 1$$

$$B = 0.2nFC\nu^{-1/6}D^{2/3}$$

where I_L is the current density ($A\ cm^{-2}$), n is the number of electrons for the reaction, F is the Faraday constant ($96,500\ C\ mol^{-1}$), D is the diffusion coefficient of O_2 in the solution ($2.0 \times 10^{-5}\ cm^2\ s^{-1}$), ν is the kinematic viscosity of the solution ($0.01\ cm^2\ s^{-1}$), C is the concentration of O_2 in the air saturated solution ($0.25\ mM$), and ω is the rotation rate (rpm). I_k is the kinetic current density for O_2 reduction and can be calculated from the intercept of the Koutecky-Levich plot. The slope for the Koutecky-Levich plot for the experimental data is very near the slope for the theoretical $n = 2$ line giving a value for $n = 2.3$, Figure 20b. Enhanced catalytic activity toward O_2 reduction by para-hydroxyphenyl substituted Co(II) porphyrins has been attributed to the electron-donating ability of these substituents.³⁶ The majority of O_2 is electrocatalytically reduced to H_2O_2 , $2e^-$ process, at the EPG electrode coated with **3** prior to oxidation of the adsorbed complex.

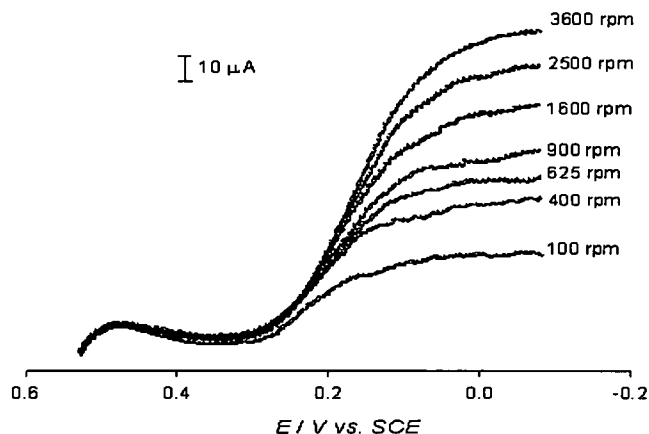


Figure 21. Current-potential curves in air saturated 1.0 M HClO_4 solution for the reduction of O_2 at a rotating disk electrode coated with complex **3** after oxidation at 1.0 V with a scan rate of 5 mV/sec.

Figure 21 illustrates the results of O_2 reduction at an EPG electrode coated with **3**, after surface oxidation, in an air saturated 1.0 M HClO_4 solution. The Levich plot reveals similar deviation from linearity related to the kinetics of $\text{Co(II)}\text{-O}_2$ bond formation, Figure 22a. The Koutecky-Levich plot of this data, Figure 22b, gives an n value of 3.3 suggesting that a significant amount of O_2 is reduced directly to H_2O at this electrochemically modified surface.

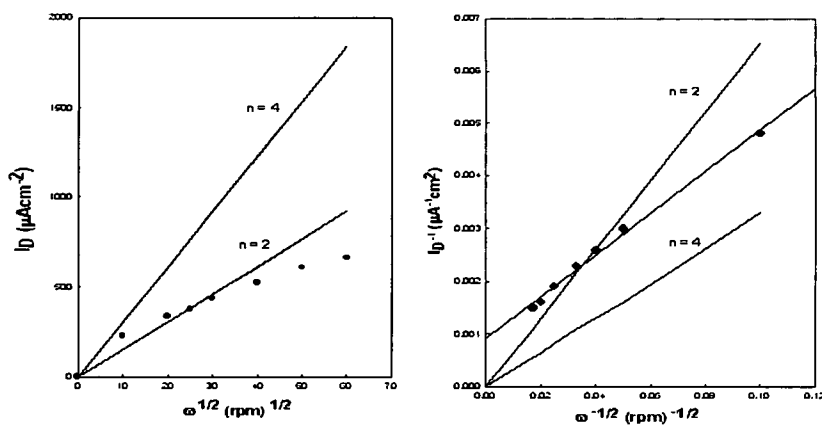


Figure 22. (a) Levich plot of plateau current vs. square root of the rotation rate for the current-potential curves of complex **3**, Figure 21. (b) Koutecky-Levich plot of the inverse of the plateau current vs. inverse of square root of the rotation rate for current-potential curves of complex **3**, Figure 21. The theoretical two electron and four electron lines are marked $n = 2$ and $n = 4$, respectively.

Analysis of the Koutecky-Levich intercept before and after oxidation of the adsorbed complex using equation 2 reveals information about the current-limiting formation of the Co-O₂ bond.

$$I_k = nFk\Gamma C_{O_2} \quad 2$$

where Γ is the surface concentration of catalyst on the electrode (mol cm⁻²) and k is the second-order rate constant associated with the current-limiting reaction between Co(II) and O₂ (M⁻¹ s⁻¹). Without a detailed understanding of the structure of the adsorbed complexes after oxidation it is difficult to determine with any certainty the surface concentration, therefore a quantitative look at the rate constant k in equation 2 is not possible. We can however determine qualitatively the effect of oxidation of complex **3** on the rate of interaction between Co(II) and O₂. The ratio of I_k^b/n , where $n = 2.3$, before oxidation to I_k^a/n , where $n = 3.3$, after oxidation gives a relationship between the rate constants k^b before and k^a after oxidation. The value for this ratio is near unity ($k^b = k^a$). This seemingly unremarkable finding indicates that the rate of formation of the Co-O₂ bond is unaffected by electrooxidation of the surface confined complex, **3**. Therefore the macrocycle core seems to be intact after oxidation. The enhanced catalytic ability resulting from oxidation of the adsorbed complex may result from formation of a more stable cobalt-peroxo interaction. The role of the oxidation as well as the resulting structure of the oxidized complex and the role of Pt(II) in the stabilization of this interaction is currently being studied.

CHAPTER IV

CONCLUSIONS

This study describes the synthesis of three new complexes, 5-(4-pyridyl)-10,15, 20-(3-methoxy-4-hydroxyphenyl)porphyrin (1), *cis*-Pt(DMSO)-[5-(4-pyridyl)-10,15,20-(3-methoxy-4-hydroxyphenyl)porphyrin]Cl₂ (2) and *cis*-Pt(DMSO)-[5-(4-pyridyl)-10,15,20-(3-methoxy-4-hydroxyphenyl)porphyrinatocobalt(II)]Cl₂ (3). The complexes were characterized by ¹H NMR, elemental analysis, UV-Vis spectroscopy and solution electrochemistry. Adsorption of these complexes onto EPG electrodes followed by oxidation in 1.0 M HClO₄ results in a new redox active modified electrode which electrocatalytically reduces O₂ to H₂O₂ and H₂O. Studies are currently underway to determine if increasing the number of Pt(II) peripheral groups will result in 100% reduction of oxygen directly to water.

CHAPTER V

FURTHER EXPERIMENTS

The current studies gave good evidence that a significant percentage of O_2 reduced at the oxidized Co(II) / Pt(II) EPG electrode was converted to H_2O as determined by rotating disk electrode measurements. Further studies are underway to synthesize a monocobalt diplatinum porphyrin to study the electrocatalytic reduction of O_2 in 1.0 M $HClO_4$ at an EPG electrode using cyclic voltammetry and rotating disk electrode (RDE) voltammetry. The proposed structure of the porphyrin for further studies is illustrated in Figure 23.

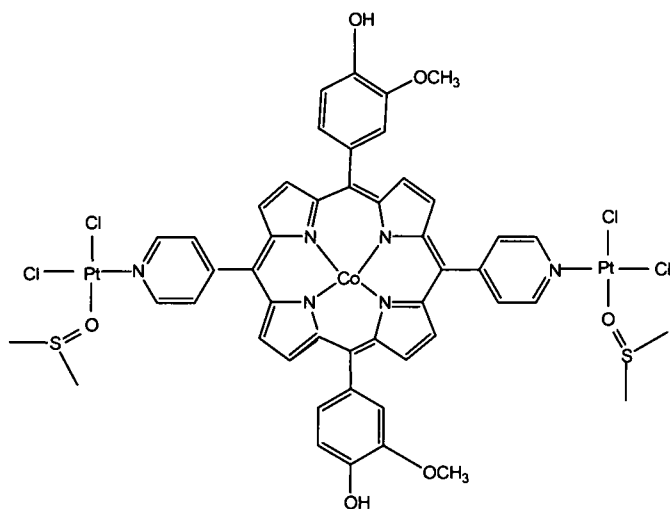


Figure 23. Proposed structure of porphyrin for further study.

CHAPTER VI
BIBLIOGRAPHY

1. Hirschenhofer, J.H.; Stauffer, D.B.; Engleman, R.R. *Fuel Cells: A Handbook* (Revision 3) **1994**, 1.
2. Azad A. M.; Larose S.; Akbar S.A. *Journal of Materials Science*, **1994** – Springer
3. Lamy, C.; Leger J. M.; Srinivasan, S. *Modern Aspects of Electrochemistry*, Kluwer Academic Publishers/Plenum Press, New York, **2001**, 53.
4. E. Yeager, **1976** in *Electroanalysis on Non-metallic Surfaces*, pp. 203, NSB Special Publication 455.
5. Bockris, J. O'M.; Srinivasan, S. *Fuel Cells: Their Electrochemistry*; McGraw-Hill Book Co.: New York, **1969**.
6. Collman, J. P.; Chng, L. L; Tyvoll, D. A. *Inorganic Chemistry* **1995**, 34, 1311.
7. Schiffrin, D. J. *Electrochemistry* **1983**, 8, 126.
8. Van Veen, J. A. R.; Van Baar, J. F. *Rev. Inorg. Chem.* **1982**, 4, 293.
9. Collman, J. P.; Denisevich, P; Konai, Y; Marrocco, M; Koval, C; Anson, F. C. *Journal of the American Chemical Society* **1980**, 102, 6027.
10. Collman, J. P.; Boulatov, R.; Sunderland, C. J. *Porphyrin Handbook* **2003**, 11, 1.
11. Fukuzumi, S *Porphyrin Handbook* **2000**, 8, 115.
12. Kadish, K. M.; Fremond, L; Burdet, F.; Barbe, J-M; Gros, C. P.; Guillard, Roger. *Journal of Inorganic Biochemistry* **2006**, 100, 858.
13. Shi, C.; Anson, F. C. *Journal of the American Chemical Society* **1991**, 113, 9564.

14. Shi, C.; Mak, K. W.; Chan, K.S.; Anson, F. C. *Journal of Electroanalytical Chemistry* **1995**, 397, 321.
15. Durand, R. R. Jr.; Bencosme, C. S.; Collman, J. P.; Anson, F. C. *Journal of the American Chemical Society* **1983**, 105, 2710.
16. Fukuzumi, S.; Okamoto, K.; Gros, C.P.; Guillard, R. *Journal of the American Chemical Society* **2004**, 126, 10441.
17. Anson, F. C.; Shi, C.; Steiger, B. *Accounts of Chemical Research* **1997**, 30, 437.
18. Shi, C. and Anson, F. C. *Inorg. Chim. Acta* **1994**, 225, 215.
19. Steiger, B. and Anson, F. C. *Inorganic chemistry* **1994**, 33, 5767.
20. Malinski, T.; Ciszewski, A.; Bennett, J.; Fish, J. R.; Czuchajowski, L. *Journal of the Electrochemical Society* **1991**, 138, 2008.
21. Bennett, J. E.; Burewicz, A.; Wheeler, D. E.; Eliezer, I.; Czuchajowski, L.; Malinski, T. *Inorganica Chimica Acta* **1998**, 271, 167.
22. Cataldi, T.R. I.; Centonze, D; Ricciardi, G. *Electroanalysis* **1995**, 7, 312.
23. Ciszewski, A. *Electroanalysis*, **1995**, 7, 1132.
24. Vago, J. M.; Dall'Orto, V. C.; Forzani, E; Hurst, J; Rezzano, I. N. *Sensors and Actuators, B*, **2003**, 96, 407.
25. Love, W. G.; Cook, M. J.; Russell, D. A. *PCT Int. Appl.* **2000**, 131.
26. Chen, S.M.; Chen, Y.L. *Journal of Electroanalytical Chemistry* **2004**, 573, 277.
27. Ojani, R.; Raoof, J. B.; Afagh, P. S. *Bulletin of Electrochemistry* **2004**, 20, 251.
28. Yeh, C.Y.; Cheng, S.H. *Journal of Science and Engineering* **2003**, 6, 81.
29. Price, J. H.; Williamson, A. N.; Schramm, R. F.; Wayland, B. B. *Inorganic Chemistry* **1972**, 11, 1280.
30. Yuan, H.; Thomas, L.; Woo, L. K. *Inorganic Chemistry* **1996**, 35, 2808.
31. Kadish, K. M.; Van Caemelbecke, E. *Journal of Solid State Electrochemistry* **2003**, 7, 254.
32. Brown, A. R.; Guo, Z.; Mosselmans, F. W. J.; Parsons, S.; Schroeder, M.; Yellowlees, L. J. *Journal of the American Chemical Society* **1998**, 120, 8805.

R002592780

33. Arullo-McAdams C., Kadish, K. M. *Inorganic chemistry* **1990**, 29, 2749.
34. Pariente, F.; Lorenzo, E.; Abruna, H. D. *Analytical Chemistry* **1994**, 66, 4337.
35. Koutecky J., Levich V. G. *Zhurnal Fizicheskoi Khimii* **1958**, 32, 1565.
36. Yuasa, M.; Steiger, B., Anson, F. C. *Journal of porphyrins Pthalocyanines* **1997**, 1, 181.